Title

Genetic and Environmental Influences on Structural and Diffusion-Based Alzheimer's Disease Neuroimaging Signatures Across Midlife and Early Old Age

Journal

Biological Psychiatry Cognitive Neuroscience and Neuroimaging, 8(9)

ISSN

2451-9022

Authors

Williams, McKenna E

Gillespie, Nathan A

Bell, Tyler R

et al.

Publication Date

2023-09-01

DOI

10.1016/j.bpsc.2022.06.007

Peer reviewed

HHS Public Access

Author manuscript

Biol Psychiatry Cogn Neurosci Neuroimaging. Author manuscript; available in PMC 2024 September 01.

Published in final edited form as:

Biol Psychiatry Cogn Neurosci Neuroimaging. 2023 September ; 8(9): 918–927. doi:10.1016/j.bpsc.2022.06.007.

Genetic and environmental influences on structural- and diffusion-based Alzheimer's disease neuroimaging signatures across midlife and early old age

McKenna E. Williams[1,2,3], **Nathan A. Gillespie**[4], **Tyler R. Bell**[1,3], **Anders M. Dale**[5,6], **Jeremy A. Elman**[1,3], **Lisa T. Eyler**[3,7], **Christine Fennema-Notestine**[3,5], **Carol E. Franz**[1,3], **Donald J. Hagler Jr.**[5], **Michael J. Lyons**[8], **Linda K. McEvoy**[5], **Michael C. Neale**[4], **Matthew S. Panizzon**[1,3], **Chandra A. Reynolds**[9], **Mark Sanderson-Cimino**[1,2,3], **William S. Kremen**[1,3]

[1]Center for Behavior Genetics of Aging, University of California San Diego, La Jolla, CA, USA

[2]Joint Doctoral Program in Clinical Psychology, San Diego State University/University of California, San Diego, CA, USA

[3]Department of Psychiatry, University of California San Diego, La Jolla, CA, USA

[4]Virginia Institute for Psychiatric and Behavior Genetics, Virginia Commonwealth University, VA, USA

[5]Department of Radiology, University of California San Diego, La Jolla, CA, USA

[6]Department of Neuroscience, University of California San Diego, La Jolla, CA, USA

[7]Desert Pacific Mental Illness Research Education and Clinical Center, VA San Diego Healthcare System, CA, USA

[8]Department of Psychological and Brain Sciences, Boston University, Boston, MA, USA

[9]Department of Psychology, University of California Riverside, Riverside, CA, USA

Abstract

Background: Composite scores of MRI-derived metrics in brain regions associated with Alzheimer's disease (AD), commonly termed 'AD signatures,' have been developed to distinguish early AD-related atrophy from normal age-associated changes. Diffusion-based gray matter signatures may be more sensitive to early AD-related changes compared to thickness/volume-based signatures, demonstrating their potential clinical utility. The timing of early (*i.e.,* midlife) changes in AD signatures from different modalities, and whether diffusion- and thickness/volume-based signatures each capture unique, AD-related phenotypic or genetic information, remains unknown.

Methods: Our validated thickness/volume signature, our novel mean diffusivity (MD) signature, and an MRI-derived measure of brain age were used in biometrical analyses to examine genetic and environmental influences on the measures, as well as phenotypic and genetic relationships between measures over 12 years. Participants were 736 men from three waves of the Vietnam Era

Corresponding author: McKenna E. Williams, M.S., Center for Behavior Genetics of Aging, University of California, San Diego, 9500 Gilman Drive (MC 0738), La Jolla, CA 92093. mewillia@health.ucsd.edu.

Twin Study of Aging (VETSA; baseline age=56.1, SD=2.6, range=51.1-60.2). Subsequent waves were at approximately 5.7-year intervals.

Results: MD and thickness/volume signatures were highly heritable (56-72%). Baseline MD signatures predicted thickness/volume signatures over a decade later, but baseline thickness/volume signatures showed a significantly weaker relationship with future MD signatures. AD signatures and brain age were correlated, but each measure captured unique phenotypic and genetic variance.

Conclusions: Cortical MD and thickness/volume AD signatures are heritable, and each signature captures unique variance that is also not explained by brain age. Moreover, results are in line with changes in MD emerging before changes in cortical thickness, underscoring the utility of MD as a very early predictor of AD risk.

Keywords

Alzheimer's disease; mean diffusivity; cortical thickness; brain age; genetics; early prediction

Introduction

Composite scores of MRI-based morphometry in brain regions associated with Alzheimer's disease (AD) pathology, commonly termed 'AD signatures', are innovative tools developed to identify brain changes specific to mild AD. These signatures are associated with AD symptom severity, AD-related biomarkers (such as β-amyloid or tau), and have been shown to predict progression to mild cognitive impairment (MCI) or AD dementia (1–8).

Most prior research has used AD signatures that rely on macrostructural neuroimaging methods (*e.g.,* cortical thickness or volume derived from structural MRI) that are unable to detect microstructural changes that may present early in the disease process. In contrast, diffusion MRI (dMRI) offers the ability to examine neural microstructure by measuring the diffusion of water molecules within particular regions (9). By providing a window into microstructural changes, dMRI metrics may serve as particularly useful early biomarkers for AD-related changes in gray matter. Mean diffusivity (MD) is one such standard dMRI metric that may reflect the microstructural integrity of neurites and cell bodies in gray matter by measuring the average water diffusion within a voxel, which increases as microstructural barriers degenerate (9).

Some evidence suggests that these microstructural changes measured using various dMRI approaches may predate macrostructural atrophy as measured using conventional structural MRI techniques (9, 10). Several studies have found increased cortical MD in individuals with MCI or AD (9, 11–14), lending support to the idea that a gray matter MD signature could provide a way of measuring very early AD-related changes. Our group recently used a cortical thickness/volume signature and a novel gray matter MD signature to predict 12-year progression to MCI among middle-aged, cognitively normal (CN) men in their 50s (15). We found that the novel MD signature significantly improved longitudinal prediction of MCI beyond prediction based on age and polygenic risk for AD, whereas the thickness/volume signature did not improve prediction. This finding was followed by work by Rodriguez-

Vieitez et al. (2021) demonstrating that elevated cortical MD predicted faster progression to MCI among older adults (average age=72.5 years, SD=9.4) over an average follow-up period of 3.2 years, but measures of cortical thickness did not predict clinical progression (16). Related results from a cross-sectional study by Vogt and colleagues (2020) showed that a composite based on multi-shell dMRI measures discriminated between CN and MCI participants better than a composite based on cortical thickness (17). Collectively, this evidence is consistent with the idea that neuropathological changes measured using dMRI emerge before changes measured using structural MRI, though it is unclear how early these changes may occur and how the two measures are related in very early disease states.

When examining multiple modalities of AD signatures (*e.g.,* structural MRI and dMRI), the issue of redundancy is raised: do different signatures capture unique information related to AD? Our group has shown that variation in cortical and subcortical gray matter MD is heritable and partly influenced by genetic factors that are distinct from genetic factors influencing cortical thickness or subcortical volumes (18, 19). Consistent with these findings, recent evidence suggests that the cross-sectional discriminative and longitudinal predictive utility of dMRI measures remains even after controlling for cortical thickness, suggesting that dMRI and structural MRI metrics may capture unique information even within the same brain regions (16, 17).

Additionally, the extent to which AD signatures measure unique neuropathological changes unexplained by general age-associated changes remains unclear. Given that Alzheimer's disease and age-associated neurodegeneration share a considerable degree of regional overlap and that age is a well-established risk factor for AD (20–23), it is possible that AD signatures could function to a large extent as indices of general aging. Previous work has demonstrated that adjusting AD signatures for age-related variance can increase (24) or does not substantively change their predictive utility (15). These findings lend support to the idea that AD signatures may capture some AD-specific variance that is distinct from measures of brain age, though the degree of variance shared between different AD signatures and brain age remains unclear.

Despite the demonstrated predictive utility of AD signatures and their potential clinical relevance, the contribution of genetic influences on these neuroimaging biomarkers are unknown. Moreover, examining the relationship between diffusion and structural AD signatures, and how this relationship may change across time, can yield insight into the predictive utility of these measures across the AD continuum. Twin modeling offers the unique opportunity to estimate genetic and environmental contributions to observed phenotypes, as well as the ability to estimate genetic, environmental, and phenotypic correlations both between and within measures across time. Here, we leveraged twin data from the Vietnam Era Twin Study of Aging (VETSA) to address the above gaps in our understanding with three key aims: 1) estimate the genetic and environmental influences on AD signatures across three timepoints; 2) test the strength of genetic and phenotypic relationships between structural and diffusion MRI signatures across a 12-year period; and 3) determine the extent to which AD signatures derived from different modalities (*e.g.,* structural and diffusion MRI) and brain age are consistent with their being genetically or phenotypically distinct neuroimaging biomarkers. We hypothesized: 1) AD signatures will

be heritable; 2) earlier MD signatures will predict later thickness/volume signature scores; and 3) genetic contributions to AD signatures will be partially independent of the genetic contributions to general brain aging.

Methods and Materials

Participants

The Vietnam Era Twin Study of Aging (VETSA) is a longitudinal study of cognitive and brain aging and risk for Alzheimer's disease beginning in middle age (25). Participants were 736 men from VETSA. This community-dwelling sample of male twins is similar to nationally representative samples of American men in their age range with respect to health and lifestyle characteristics (26). All served in the United States military at some point between 1965 and 1975. Approximately 80% reported no combat exposure. The study was approved by the Institutional Review Boards at the University of California, San Diego (UCSD), Boston University, and the Massachusetts General Hospital (MGH). Written informed consent was obtained from all participants.

MRI acquisition and processing

Images at wave 1 (baseline) were acquired on Siemens 1.5T scanners at UCSD and MGH. Images at wave 2 were acquired with a GE 3T Discovery 750x scanner (GE Healthcare, Waukesha, WI, USA) with an 8-channel phased array head coil at UCSD and with a Siemens Tim Trio (Siemens USA, Washington, D.C.) with a 32-channel head coil at MGH. Images at wave 3 were acquired at UCSD with two GE 3T Discovery 750x scanners with eight-channel phased array head coils. Volumetric segmentation (27, 28) and cortical surface reconstruction (27–30) methods were performed with FreeSurfer version 5.1 (http://surfer.nmr.mgh.harvard.edu). Structural (27–32) and diffusion (18, 19) MR images were processed as described previously and are available in supplementary materials.

Alzheimer's disease brain signatures and predicted brain age difference scores

We used an AD brain signature that was previously developed by our group using data from the Alzheimer's Disease Neuroimaging Initiative (6, 7). This signature (Figure 1) is a weighted average of thickness in seven cortical regions plus hippocampal volume, with separate weights for left and right hemisphere regions (referred to as "thickness/volume signature"). For the structural and diffusion data, we regressed out effects of age and scanner for each ROI, as well as estimated intracranial volume for the hippocampus to control for differences in head size, which affect volume but not thickness measures. Standardized residuals of ROIs were then weighted accordingly and summed together to form the thickness/volume signature scores. Given that there is, as yet, no independently created AD gray matter MD signature (referred to as "MD signature"), we applied these same weightings to the MD values for each ROI and carried out the same steps to generate our novel MD signature scores.

Predicted brain age was estimated using the Brain-Age Regression Analysis and Computation Utility software BARACUS v0.9.4 (33). We focused on predicted brain age difference (PBAD) scores, which have demonstrated stronger associations with cognition

when compared to predicted brain age (33). PBAD scores were calculated by subtracting predicted brain age from the chronological age. A negative PBAD is indicative of brain age estimated to be older than one's chronological age (34–36). All PBAD scores were adjusted for scanner type prior to analyses.

Statistical analysis

Multivariate biometrical models were performed using maximum likelihood estimation in the OpenMx$_{2.17.4}$(37) software package in R$_{3.4.1}$(38). Two outliers in the MD signature data that were more than four times the interquartile range below the first quartile were excluded from analyses. Prior to twin modeling all PBAD and signature scores were residualized for the effects of race and ethnicity using the umx_residualize() function in the umx software package, version 4.9.0 (39).

In the biometrical 'ACE' models, the total variance in each measure is decomposed into additive genetic (A) influences, shared or common environmental (C) influences (i.e., environmental factors that make members of a twin pair similar to one another), and non-shared or unique environmental (E) influences (i.e., environmental factors that make members of a twin pair different from one another). The decomposition is achieved by exploiting the expected genetic and environmental correlations among monozygotic (MZ) and dizygotic (DZ) twin pairs (see Figure 2). MZ twin pairs are genetically identical, whereas DZ twin pairs share, on average, half of their segregating genes. Therefore, the MZ and DZ twin pair correlations for the additive genetic effects are fixed to r_A=1.0 and r_A=0.5, respectively. The model assumes that common environmental effects (C) are equal in MZ and DZ twin pairs (r_C=1.0), while non-shared environmental effects (E) are by definition uncorrelated and include measurement error. The proportion of the overall variance in a phenotype that is attributable to additive genetic influences is the heritability (40, 41).

Importantly, these A, C, and E components of the twin model are latent variables. These models do not address the number of genes, type of genes, or specific environmental factors. Rather, these models estimate the total amount of variance in the measures that can be attributable to genetic or environmental factors. For example, suppose the correlation of a trait in MZ twin pairs is 0.75. Given MZ twins share all of their genes and all of the common environment, this correlation (shared variance) must be due to a combination of A and C components. Based on this correlation alone, we cannot determine what proportion is due to A or C specifically. However, we can determine that the remaining non-shared portion of the variance must be due to unique environmental influences (E), even without knowing what those specific environmental factors are.

Multivariate ACE models have the capability of estimating the size and significance of genetic and environmental influences within and between each AD signature over time. To address our first two aims, we fit a multivariate correlated liabilities model with both AD signatures at each of the three VETSA waves (Figure 3). To determine the extent to which AD signatures comprising different modalities and brain age constitute distinct imaging phenotypes (aim 3), we fit separate trivariate correlated liabilities models to the estimates of the MD signature scores, thickness/volume signature scores, and PBAD scores from each of the three waves.

The fits of univariate and multivariate ACE models were tested relative to the fits of fully saturated models. The best-fitting models were determined based on an optimal balance of complexity and explanatory power using Akaike's Information Criterion (AIC), root mean square error of approximation (RMSEA), comparative fit index (CFI), and likelihood ratio chi-square tests (LRTs). For each best-fitting model, the parameters were then successively fixed to zero and their significance determined using LRTs. Univariate tests of mean and variance homogeneity (Supplemental Tables S1–S2) indicated that the data did not violate critical assumptions of the ACE model.

Results

Participants were 56.2 (SD=2.6) years old at wave 1 with an average education of 13.83 (SD=2.07, range=8-20) years. The sample consisted of men who self-identified as American Indian (<1%), Black or African American (6.3%), multiracial (1.2%), and White (91.8%). Most (96.3%) were non-Hispanic. Table 1 contains descriptive statistics and cross-twin polyserial correlations for each AD signature and PBAD.

All analyses revealed that estimates of the common environment were at or near zero and that AE models best fit the data (Supplementary Tables S4–S5). Therefore, AE models were used to estimate additive genetic (A) and non-shared environmental (E) influences for all measures. Model fitting results are further detailed in supplementary materials.

Aim 1: Heritability of AD signatures and genetic stability over time

Both AD signatures were highly heritable. Additive genetic influences accounted for between 56% to 72% of the variance in MD signature scores at each of the three waves and between 63% to 69% of the variance in thickness/volume signature scores (Table 2).

We examined the relative stability of genetic and environmental influences on each signature across time by testing phenotypic, genetic, and environmental correlations across time *within* each modality. Overall, cross-temporal phenotypic (Figure 4) and genetic correlations (Table 3) for the MD signature and for the thickness/volume signature were high, ranging from 0.59 to 0.79 (phenotypic correlations) and 0.77 to 0.98 (genetic correlations). These high correlations suggest that many of the same genes are influencing signature scores across time. Cross-temporal non-shared environmental correlations for the MD signature were small-to-moderate, suggesting the presence of some environmental influences on each signature that are consistent across waves. Any degree of measurement error is also captured by non-shared environmental influences, and correlated measurement error that similarly affects both structural and diffusion imaging modalities may also partially account for these moderate non-shared environmental correlations.

Aim 2: Relationship between MD and thickness/volume signature scores across 12 years

Next, we tested the hypothesis that earlier MD signature scores predicted later thickness/volume signature scores by examining cross-wave correlations between the two signatures. Overall, our results supported this hypothesis. Phenotypically, MD signature scores at wave 1 were significantly associated with thickness/volume signature scores at waves 2 and 3 (Figure 4). In contrast, thickness/volume signature scores at wave 1 displayed a significantly

lower correlation with MD signature scores at waves 2 and 3, as evidenced by the non-overlapping confidence intervals. However, thickness/volume signature scores at wave 2 were moderately associated with MD signature scores at wave 3, similar to the moderate association between MD signature scores at wave 2 and thickness/volume signature scores at wave 3. Cross-wave genetic correlations supported this phenotypic pattern (Table 4).

Phenotypically, within-wave correlations between the MD and thickness/volume signature scores were significantly lower at wave 1 ($r = -0.28$) compared to waves 2 ($r = -0.55$) and 3 ($r = -0.59$). Within-wave genetic correlations followed a similar pattern.

The cortical regions used in both signatures were selected a priori (6), though it may be the case that different regions drive associations in the MD signature compared to the thickness/volume signature. In post-hoc analyses, we examined correlations between individual regions in each signature at wave 1 with the cross-modal AD signature at wave 3 (Table 5). Interestingly, we found that for the thickness/volume signature regions at wave 1, only the superior temporal gyrus and hippocampus showed small-to-moderate correlations with the MD signature at wave 3. In contrast, for wave 1 MD, several regions demonstrated moderate correlations with the thickness/volume signature at wave 3, with stronger correlations among regions that are typically affected later in the disease (*e.g.* lateral orbital frontal cortex), and weaker correlations in those that are affected at the earliest stages (entorhinal cortex and hippocampus).

Aim 3: Relationship between AD signatures and brain age

Finally, we examined the extent to which AD signatures provide information that is independent of general brain aging. At wave 1, phenotypic correlations among the three phenotypes (the two AD signatures and PBAD) were moderate but significant, ranging from −0.49 to 0.27. Genetic correlations were similar, ranging from −0.62 to 0.35. At waves 2 and 3, phenotypic and genetic correlations were higher. At each wave, genetic correlations among these three measures significantly differed from r=1, indicating some degree of independent genetic contributions to the MD signature, thickness/volume signature, and PBAD.

Discussion

Our results are consistent with both structural- and diffusion-based AD signatures being highly heritable, with genetic variance accounting for approximately two-thirds of the variance in each signature score. Correlations between the two signatures are in line with earlier MD signature scores predicting later thickness/volume signature scores, but not the reverse. Moreover, our findings suggest that each AD signature captures unique genetic and phenotypic variance.

The MD and thickness/volume signatures showed similar, high heritability estimates, ranging from 56-72% across waves. This is in line with literature demonstrating many MRI measures of brain structure are heritable and show no significant effects of common environmental influences (18, 19, 31, 42–44). We also found that genetic correlations within each signature were high across the three VETSA waves, suggesting that many—or most—

of the same genes are influencing each signature across these three timepoints. Notably, our sample spans 51 to 73 years of age, a range that is much younger than many studies of AD risk factors or AD signatures (1–8, 45). Our group previously demonstrated the predictive utility of the gray matter MD signature for incident MCI among cognitively normal adults in their 50s (15). The finding that this MD signature captures substantial genetic variance that is consistent throughout midlife and into early old age supports the utility of the MD signature as a very early AD-related neuroimaging biomarker.

We found that early differences in MD signatures predict later inter-individual differences in thickness/volume signatures, but not the reverse. Prior evidence suggests that microstructural changes measured using MD may emerge earlier than macrostructural changes measured using cortical thickness or volume (9, 10). Our results are consistent with this and suggest that the predictive utility of these AD signatures can change as a function of age or disease state, such that the MD signature may capture very early, AD-related changes that are later reflected in the thickness/volume signature. Interestingly, by wave 2, the thickness/volume signature appears to have caught up with the MD signature in terms of predictive ability for future cross-modal signatures. It may be that MD is able to detect microstructural changes first, but once macrostructural changes are apparent in measures of thickness/volume, they progress at similar rates allowing each to predict the other.

Previous work from our group demonstrated that gray matter MD is influenced by genetic factors that are distinct from factors influencing cortical thickness or subcortical volumes (18, 19). Here, within-wave genetic correlations between the gray matter MD and thickness/volume signatures were small at wave 1 and moderate at waves 2 and 3. Despite the two signatures being derived from the same ROIs, our findings show that each signature contributes independent information during middle age and into older age. These results are further supported by the pattern of correlations between individual ROIs used in the signatures at wave 1 with cross-modal signatures at wave 3 (Table 5). Several wave 1 MD regions were moderately associated with the thickness/volume signature at wave 3, whereas only the superior temporal gyrus and hippocampal regions in wave 1 cortical thickness showed small-to-moderate associations with wave 3 MD signatures. This pattern emphasizes findings that the signatures capture unique phenotypic and genetic information, which may reflect different disease stages or different underlying processes. However, over time, these signatures come under the influence of more common genetic factors. This may reflect the MD signature detecting disease-related variance at earlier ages, with the thickness/volume signature “catching up” over time.

Late-onset AD, the most common form of the disease, is estimated to be 56–79% heritable (46). Genome-wide association studies (GWAS) have identified over 50 risk loci for AD. Beyond these identified risk loci, an estimated 60% of the genetic variance in late-onset AD remains unaccounted for, highlighting the complexity of the disease that can involve epistatic and polygenic mechanisms (46, 47). Many environmental factors linked to AD risk throughout the lifecourse have also been identified (48). Our twin models cannot determine how many or which genes influence AD signatures, but unlike GWAS, they are able to provide better estimates of the total genetic variance and total shared genetic variance across

different phenotypes. They also explain analogous variance components for environmental influences. These results thus provide useful complementary information to GWAS.

Findings from our study should be interpreted in the context of a few limitations. First, inferences about the process underpinning longitudinal change in AD signature scores across age are limited due to scanner differences across waves. To address this, signature scores were adjusted for scanner type and were z-scored at each wave. Additionally, the BARACUS algorithm used to calculate PBAD was developed using 3T data, whereas PBAD scores from wave 1 in the present study were based on scans conducted on 1.5T scanners. However, evidence from prior work strongly suggests that the PBAD scores in the present study are valid (34–36, 49). Additionally, the unit of measurement in twin models is within-pair correlations, and twin pairs were always scanned on the same scanner (34–36, 49).

Cortical MD is vulnerable to partial voluming effects due to the proximity to CSF. While differences in MD could reflect microstructural changes to the integrity of neurites and cell bodies, cortical MD may also be a sensitive measure of cortical thinning due to partial voluming effects (18, 50). In the latter case, increased contributions of signal from CSF due to subtle cortical thinning would result in increased MD values. To minimize this contribution, we utilize a method to weight cortical MD values based on the fraction of gray matter tissue in each sample, and our recent findings suggest that partial volume effects may not be driving observed differences in the MD signature (15). Moreover, results from the current study provide further support that the MD and thickness/volume signatures constitute partially distinct imaging phenotypes.

Without biomarker evidence, we cannot determine the extent to which variation in these signatures is driven by AD-related pathological burden. However, our results showing that each signature captured unique genetic variance unrelated to a measure of brain age strongly suggests that these AD signatures are not functioning simply as alternative measures of general brain aging. Moreover, cortical thickness AD signatures have demonstrated associations with AD symptom severity and AD-related biomarkers (1–8), supporting the idea that the genetic variance captured by the signatures in the present study may be AD-related.

The VETSA sample comprises only men and is largely White and non-Hispanic. Given evidence of differences in AD prevalence, manifestation, risk factors, and biomarkers across sex/gender and racial/ethnic groups (22, 51–53), findings may not generalize to women or individuals with different racial or ethnic backgrounds. Despite this generalizability limitation, the VETSA sample is unique in that it is a genetically informative twin study with longitudinal MRI data, and participants are very similar to American men in their age range with respect to health, lifestyle, and education characteristics (26).

To our knowledge, this is the first study to examine genetic and environmental influences on AD signatures. We found that cortical MD and cortical thickness/volume signatures are highly heritable, and each signature captures unique phenotypic and genetic variance that is also not explained by general brain aging. Previous studies have largely focused on AD signatures based on cortical thickness. Our finding that each signature contributes

unique information, even among the same ROIs, establishes the value of studying both structural- and diffusion-based signatures as early markers of AD risk beginning in middle age. MD signature scores were robustly associated with thickness/volume signature scores over a decade later, but not the reverse, supporting the idea that AD-related changes in MD may emerge before changes in cortical thickness. Moreover, this MD signature explains substantial genetic variance that is consistent throughout midlife and into early old age, supporting the potential utility of the MD signature as a very early AD-related neuroimaging biomarker that could aid in clinical trials of interventions designed to prevent AD dementia. Future work may benefit from using AD signatures as phenotypes in genetic association studies to help identify additional genetic risk factors, as well as from examining how cortical MD and cortical thickness/volume signatures may be used together to better predict risk for AD.

Supplementary Material

Refer to Web version on PubMed Central for supplementary material.

Acknowledgements

We would like to acknowledge the continued cooperation and participation of the members of the VET Registry and their families. This work was supported by National Institute on Aging R01 AG018386 (W.S.K.), AG022381 (W.S.K.), AG022982 (W.S.K.), AG050595 (W.S.K., C.E.F., M.J.L.), R01 AG018384 (M.J.L.), R03 AG046413 (C.E.F), and K08 AG047903 (M.S.P), and the VA San Diego Center of Excellence for Stress and Mental Health. The content is the responsibility of the authors and does not necessarily represent official views of the NIA, NIH, or VA. The Cooperative Studies Program of the U.S. Department of Veterans Affairs provided financial support for development and maintenance of the Vietnam Era Twin Registry.

Disclosures

L.K.M. holds stock in CorTechs Laboratories, Inc. A.M.D. is a founder and holds equity in CorTechs Laboratories, Inc. and also serves on its Scientific Advisory Board. He is a member of the Scientific Advisory Board of Human Longevity, Inc. and receives funding through research agreements with General Electric Healthcare and Medtronic, Inc. The terms of this arrangement have been reviewed and approved by the University of California, San Diego, in accordance with its conflict of interest policies. No other disclosures were reported.

References

1. Bakkour A, Morris JC, Wolk DA, Dickerson BC (2013): The effects of aging and Alzheimer's disease on cerebral cortical anatomy: specificity and differential relationships with cognition. Neuroimage. 76:332–344. [PubMed: 23507382]
2. Bakkour A, Morris JC, Dickerson BC (2009): The cortical signature of prodromal AD. Neurology. 72:1048–1055. [PubMed: 19109536]
3. Dickerson BC, Bakkour A, Salat DH, Feczko E, Pacheco J, Greve DN, et al. (2009): The cortical signature of Alzheimer's disease: regionally specific cortical thinning relates to symptom severity in very mild to mild AD dementia and is detectable in asymptomatic amyloid-positive individuals. Cereb Cortex. 19:497–510. [PubMed: 18632739]
4. Dickerson BC, Stoub TR, Shah RC, Sperling RA, Killiany RJ, Albert MS, et al. (2011): Alzheimer-signature MRI biomarker predicts AD dementia in cognitively normal adults. Neurology. 76:1395–1402. [PubMed: 21490323]
5. Dickerson BC, Wolk DA (2012): MRI cortical thickness biomarker predicts AD-like CSF and cognitive decline in normal adults. Neurology. 78:84–90. [PubMed: 22189451]
6. McEvoy LK, Fennema-Notestine C, Cooper Roddey J, Hagler DJ, Holland D, Karow DS, et al. (2009): Quantitative Structural Neuroimaging for Detection and Prediction of Clinical and Structural Changes in Mild Cognitive Impairment. Radiology. 251:195–205. [PubMed: 19201945]

7. McEvoy LK, Holland D, Hagler DJ, Fennema-Notestine C, Brewer JB, Dale AM (2011): Baseline and Longitudinal Structural MR Imaging Measures Improve Predictive Prognosis. Radiology. 259:834–843. [PubMed: 21471273]
8. Sabuncu MR, Desikan RS, Sepulcre J, Yeo BT, Liu H, Schmansky NJ, et al. (2011): The Dynamics of Cortical and Hippocampal Atrophy in Alzheimer Disease. Arch Neurol. 68:1040–1048. [PubMed: 21825241]
9. Weston PS, Simpson IJ, Ryan NS, Ourselin S, Fox NC (2015): Diffusion imaging changes in grey matter in Alzheimer's disease: a potential marker of early neurodegeneration. Alzheimers Res Ther. 7:47. [PubMed: 26136857]
10. Kantarci K (2005): Magnetic resonance markers for early diagnosis and progression of Alzheimer's disease. Expert Rev Neurother. 5:663–670. [PubMed: 16162090]
11. Fellgiebel A, Wille P, Muller MJ, Winterer G, Scheurich A, Vucurevic G, et al. (2004): Ultrastructural hippocampal and white matter alterations in mild cognitive impairment: a diffusion tensor imaging study. Dement Geriatr Cogn Disord. 18:101–108. [PubMed: 15087585]
12. Ray KM, Wang H, Chu Y, Chen Y, Bert A, Hasso AN, et al. (2006): Apparent Diffusion Coefficient in Regional Gray Matter and White Matter Structures. Radiology. 241:197–205. [PubMed: 16990677]
13. Scola E, Bozzali M, Agosta F, Magnani G, Franceschi M, Sormani MP, et al. (2010): A diffusion tensor MRI study of patients with MCI and AD with a 2-year clinical follow-up. J Neurol Neurosurg Psychiatry. 81:798–805. [PubMed: 20392973]
14. Rose SE, Janke AL, Chalk JB (2008): Gray and white matter changes in Alzheimer's disease: a diffusion tensor imaging study. J Magn Reson Imaging. 27:20–26. [PubMed: 18050329]
15. Williams ME, Elman JA, McEvoy LK, Andreassen OA, Dale A, Eglit GML, et al. (2021): 12-year prediction of mild cognitive impairment aided by Alzheimer's brain signatures at mean age 56. Brain Communications.
16. Rodriguez-Vieitez E, Montal V, Sepulcre J, Lois C, Hanseeuw B, Vilaplana E, et al. (2021): Association of cortical microstructure with amyloid-beta and tau: impact on cognitive decline, neurodegeneration, and clinical progression in older adults. Mol Psychiatry.
17. Vogt NM, Hunt JF, Adluru N, Dean DC, Johnson SC, Asthana S, et al. (2020): Cortical Microstructural Alterations in Mild Cognitive Impairment and Alzheimer's Disease Dementia. Cereb Cortex. 30:2948–2960. [PubMed: 31833550]
18. Elman JA, Panizzon MS, Hagler DJ Jr., Fennema-Notestine C, Eyler LT, Gillespie NA, et al. (2017): Genetic and environmental influences on cortical mean diffusivity. Neuroimage. 146:90–99. [PubMed: 27864081]
19. Gillespie NA, Neale MC, Hagler DJ Jr., Eyler LT, Fennema-Notestine C, Franz CE, et al. (2017): Genetic and environmental influences on mean diffusivity and volume in subcortical brain regions. Hum Brain Mapp. 38:2589–2598. [PubMed: 28240386]
20. Brookmeyer R, Gray S, Kawas C (1998): Projections of Alzheimer's Disease in the United States and the Public Health Impact of Delaying Disease Onset. American Journal of Public Health. 88:1337–1342. [PubMed: 9736873]
21. Brookmeyer R, Johnson E, Ziegler-Graham K, Arrighi HM (2007): Forecasting the global burden of Alzheimer's disease. Alzheimers Dement. 3:186–191. [PubMed: 19595937]
22. Hebert LE, Weuve J, Scherr PA, Evans DA (2013): Alzheimer disease in the United States (2010–2050) estimated using the 2010 census. Neurology. 80:1778–1783. [PubMed: 23390181]
23. Riedel BC, Thompson PM, Brinton RD (2016): Age, APOE and sex: Triad of risk of Alzheimer's disease. J Steroid Biochem Mol Biol. 160:134–147. [PubMed: 26969397]
24. Racine AM, Brickhouse M, Wolk DA, Dickerson BC, Alzheimer's Disease Neuroimaging I (2018): The personalized Alzheimer's disease cortical thickness index predicts likely pathology and clinical progression in mild cognitive impairment. Alzheimers Dement (Amst). 10:301–310. [PubMed: 29780874]
25. Kremen WS, Franz CE, Lyons MJ (2013): VETSA: the Vietnam Era Twin Study of Aging. Twin Res Hum Genet. 16:399–402. [PubMed: 23110957]
26. Schoeneborn CA, Heyman KM (2009): Health characteristics of adults aged 55 years and over: United States, 2004–2007. National Health Statistics Report; no 16.

27. Fischl B, Salat DH, Busa E, Albert M, Dieterich M, Haselgrove C, et al. (2002): Whole Brain Segementation: Automated Labeling of Neuroanatomical Structures in the Human Brain. Neuron. 33:341–355. [PubMed: 11832223]
28. Fischl B, van der Kouwe A, Destrieux C, Halgren E, Segonne F, Salat DH, et al. (2004): Automatically parcellating the human cerebral cortex. Cereb Cortex. 14:11–22. [PubMed: 14654453]
29. Dale AM, Sereno MI (1993): Improved Localizadon of Cortical Activity by Combining EEG and MEG with MRI Cortical Surface Reconstruction: A Linear Approach. J Cogn Neurosci. 5:162–176. [PubMed: 23972151]
30. Dale AM, Fischl B, Sereno MI (1999): Cortical surface-based analysis. I. Segmentation and surface reconstruction. Neuroimage. 9:179–194. [PubMed: 9931268]
31. Kremen WS, Prom-Wormley E, Panizzon MS, Eyler LT, Fischl B, Neale MC, et al. (2010): Genetic and environmental influences on the size of specific brain regions in midlife: the VETSA MRI study. Neuroimage. 49:1213–1223. [PubMed: 19786105]
32. McEvoy LK, Fennema-Notestine C, Eyler LT, Franz CE, Hagler DJ Jr., Lyons MJ, et al. (2015): Hypertension-related alterations in white matter microstructure detectable in middle age. Hypertension. 66:317–323. [PubMed: 26056337]
33. Liem F, Varoquaux G, Kynast J, Beyer F, Kharabian Masouleh S, Huntenburg JM, et al. (2016).
34. Hatton SN, Franz CE, Elman JA, Panizzon MS, Hagler DJ Jr., Fennema-Notestine C, et al. (2018): Negative fateful life events in midlife and advanced predicted brain aging. Neurobiol Aging. 67:1–9. [PubMed: 29609076]
35. Franz CE, Hatton SN, Elman JA, Warren T, Gillespie NA, Whitsel NA, et al. (2021): Lifestyle and the aging brain: interactive effects of modifiable lifestyle behaviors and cognitive ability in men from midlife to old age. Neurobiol Aging. 108:80–89. [PubMed: 34547718]
36. Whitsel N, Reynolds CA, Buchholz EJ, Pahlen S, Pearce RC, Hatton SN, et al. (2021): Long-term associations of cigarette smoking in early mid-life with predicted brain aging from mid- to late life. Addiction.
37. Boker S, Neale M, Maes H, Wilde M, Spiegel M, Brick T, et al. (2011): OpenMx: An Open Source Extended Structural Equation Modeling Framework. Psychometrika. 76:306–317. [PubMed: 23258944]
38. Team RC (2020).
39. Bates TC, Neale MC, Maes HH (2019): umx: A library for Structural Equation and Twin Modelling in R. Twin Research and Human Genetics. 22:27–41. [PubMed: 30944056]
40. Neale MC, Cardon LR (1992). Dordrecht, The Netherlands: Kluwer Academics Publishers.
41. Eaves LJ, Last KA, Young PA, Martin NG (1978): Model-fitting approaches to the analysis of human behavior. Heredity. 41:249–320. [PubMed: 370072]
42. Blokland GA, de Zubicaray GI, McMahon KL, Wright MJ (2012): Genetic and environmental influences on neuroimaging phenotypes: a meta-analytical perspective on twin imaging studies. Twin Res Hum Genet. 15:351–371. [PubMed: 22856370]
43. Chiang MC, Barysheva M, Shattuck DW, Lee AD, Madsen SK, Avedissian C, et al. (2009): Genetics of brain fiber architecture and intellectual performance. J Neurosci. 29:2212–2224. [PubMed: 19228974]
44. Eyler LT, Prom-Wormley E, Panizzon MS, Kaup AR, Fennema-Notestine C, Neale MC, et al. (2011): Genetic and environmental contributions to regional cortical surface area in humans: a magnetic resonance imaging twin study. Cereb Cortex. 21:2313–2321. [PubMed: 21378112]
45. Putcha D, Brickhouse M, O'Keefe K, Sullivan C, Rentz D, Marshall G, et al. (2011): Hippocampal hyperactivation associated with cortical thinning in Alzheimer's disease signature regions in non-demented elderly adults. J Neurosci. 31:17680–17688. [PubMed: 22131428]
46. Sims R, Hill M, Williams J (2020): The multiplex model of the genetics of Alzheimer's disease. Nat Neurosci. 23:311–322. [PubMed: 32112059]
47. Raghavan N, Tosto G (2017): Genetics of Alzheimer's Disease: the Importance of Polygenic and Epistatic Components. Curr Neurol Neurosci Rep. 17:78. [PubMed: 28825204]

48. Livingston G, Huntley J, Sommerlad A, Ames D, Ballard C, Banerjee S, et al. (2020): Dementia prevention, intervention, and care: 2020 report of the Lancet Commission. The Lancet. 396:413–446.

49. Gillespie NA, Hatton SN, Hagler DH, Dale AM, Elman JA, McEvoy LK, et al. (2021): The genetic etiology of longitudinal measures of predicted brain ageing in a population-based sample of mid to late-age males. bioRxiv.

50. Koo BB, Hua N, Choi CH, Ronen I, Lee JM, Kim DS (2009): A framework to analyze partial volume effect on gray matter mean diffusivity measurements. Neuroimage. 44:136–144. [PubMed: 18775785]

51. Tang M-X, Cross P, Andrews H, Jacobs DM, Small S, Bell K, et al. (2001): Incidence of AD in African-Americans, Caribbean Hispanics, and Caucasians in northern Manhattan. Neurology. 56:49–56. [PubMed: 11148235]

52. Ferretti MT, Iulita MF, Cavedo E, Chiesa PA, Schumacher Dimech A, Santuccione Chadha A, et al. (2018): Sex differences in Alzheimer disease - the gateway to precision medicine. Nat Rev Neurol. 14:457–469. [PubMed: 29985474]

53. Royse SK, Cohen AD, Snitz BE, Rosano C (2021): Differences in Alzheimer's Disease and Related Dementias Pathology Among African American and Hispanic Women: A Qualitative Literature Review of Biomarker Studies. Front Syst Neurosci. 15:685957. [PubMed: 34366799]

54. Bondi MW, Edmonds EC, Jak AJ, Clark LR, Delano-Wood L, McDonald CR, et al. (2014): Neuropsychological criteria for mild cognitive impairment improves diagnostic precision, biomarker associations, and progression rates. J Alzheimers Dis. 42:275–289. [PubMed: 24844687]

55. Bondi MW, Jak AJ, Delano-Wood L, Jacobson MW, Delis DC, Salmon DP (2008): Neuropsychological contributions to the early identification of Alzheimer's disease. Neuropsychol Rev. 18:73–90. [PubMed: 18347989]

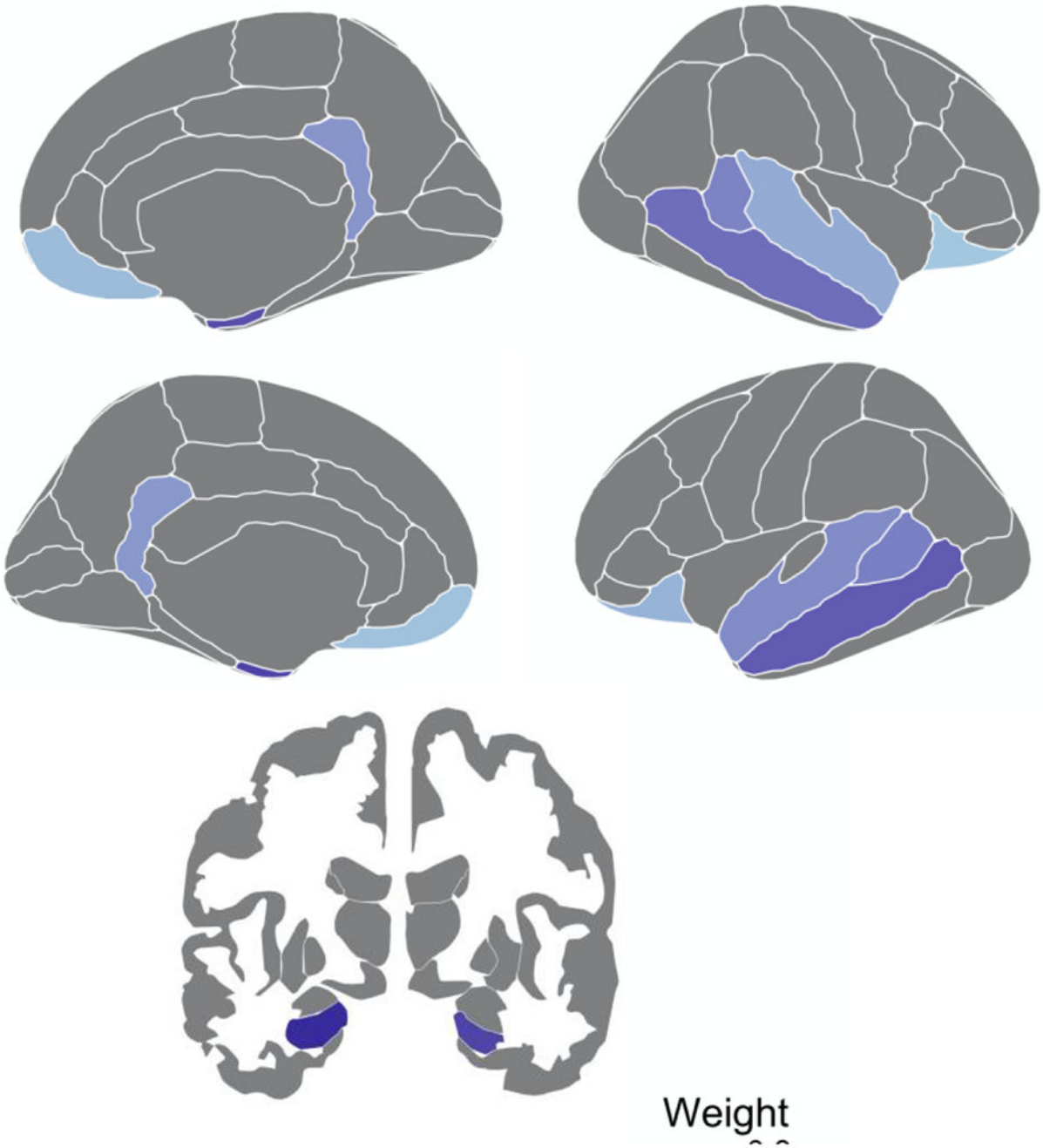

Figure 1. Regions and corresponding weights used to create AD signatures.

The cortical thickness/volume signature is a weighted average of thickness in seven cortical regions (entorhinal cortex, middle temporal gyrus, bank of superior temporal sulcus, superior temporal gyrus, isthmus cingulate, lateral orbitofrontal cortex, and medial orbitofrontal cortex) plus hippocampal volume, with separate weights for left and right hemisphere regions. We applied the same weightings to MD values for each of these ROIs to generate our novel MD signature scores.

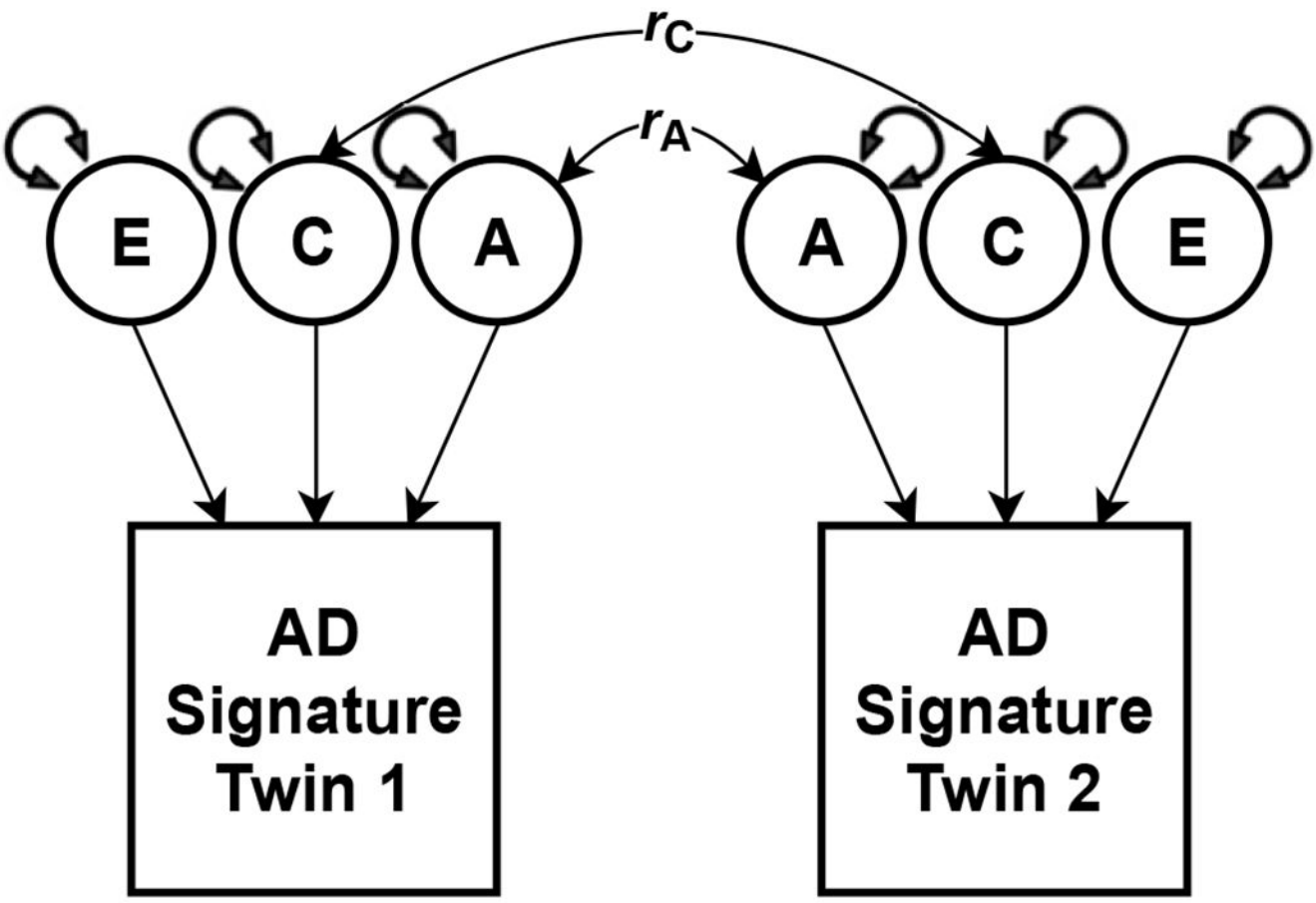

Figure 2.
Univariate variance decomposition to estimate the relative contribution of genetic and environmental influences on AD signatures. A=additive genetic, C=common/shared environmental, and E=unique environmental influences. r_C=correlation of 1 for MZ and DZ twin pairs, r_A=correlations 1 for MZ and 0.5 for DZ twin pairs.

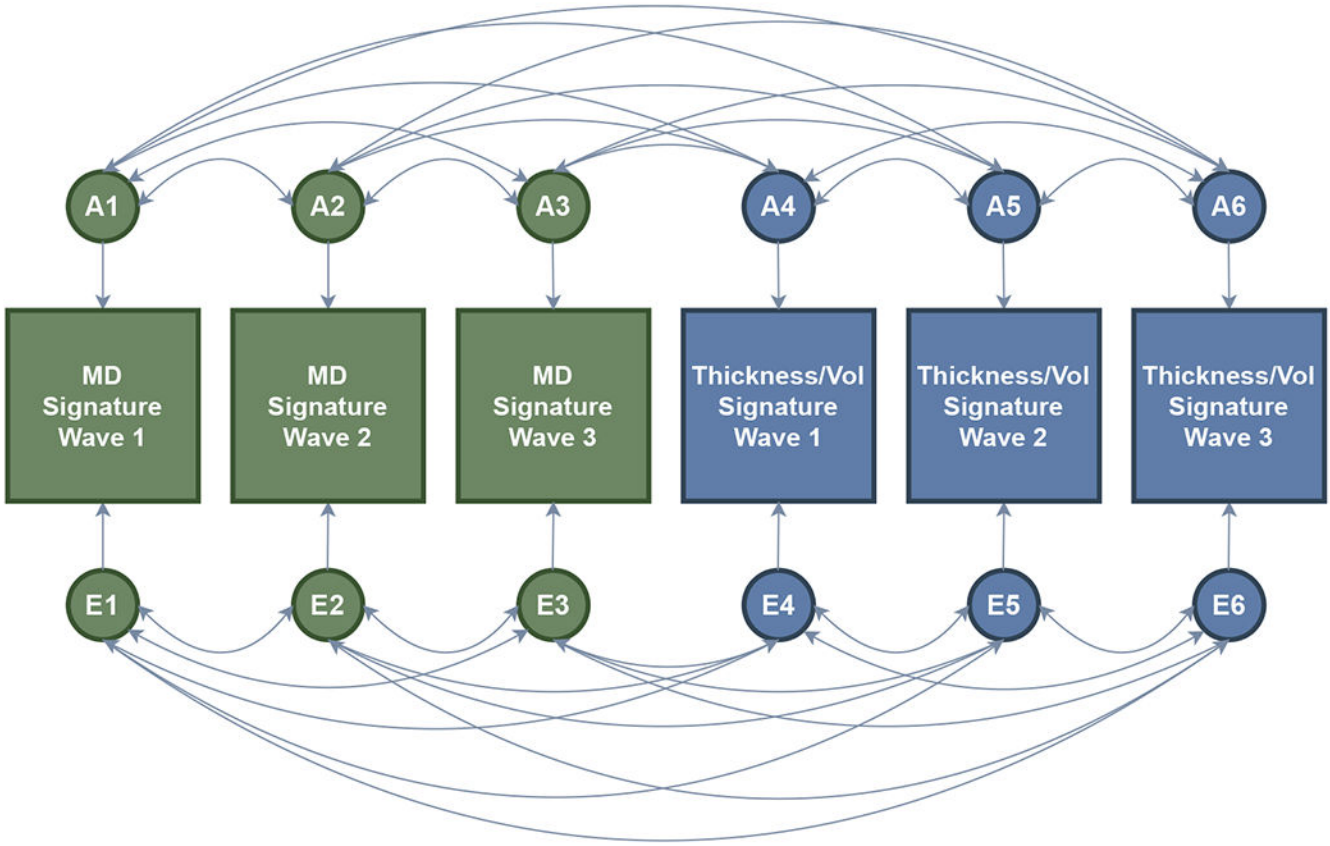

Figure 3. Multivariate correlated liabilities model with both AD signatures.

This model allows for the estimation of the phenotypic, genetic, and environmental correlations both within and between AD signatures across waves, without the assumption of any underlying factor structure for each signature. Correlation estimates from this model were used to address aim 2. For brevity, only additive genetic (A) and unique environmental (E) influences are shown (common environmental influences and autocorrelations are omitted).

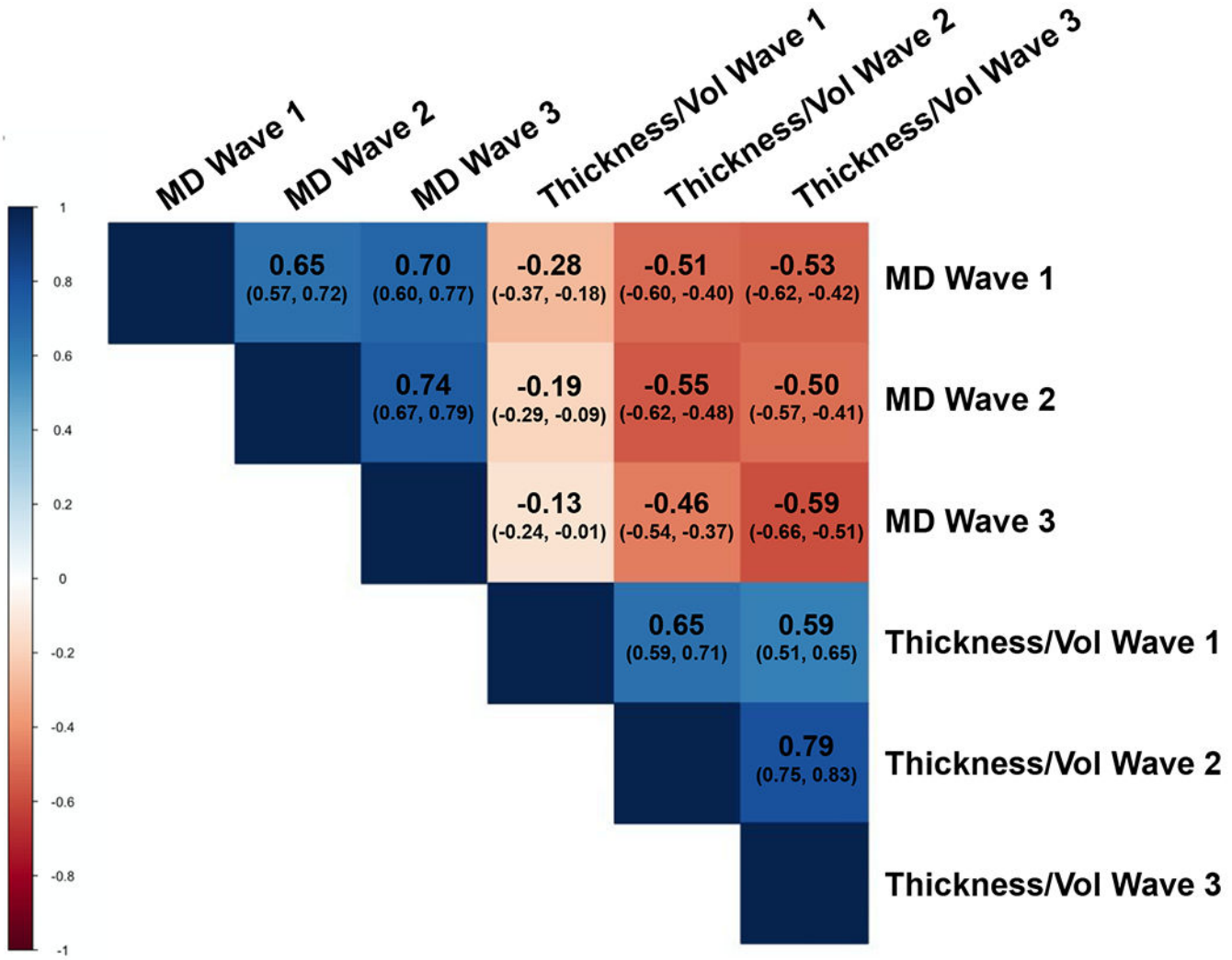

Figure 4. Phenotypic correlations from best-fitting multivariate correlated liabilities model.
Mean diffusivity (MD) and cortical thickness/volume signatures phenotypic correlations (and 95% confidence intervals).

Table 1.

Descriptive statistics. Mean diffusivity (MD) signature, cortical thickness/volume signature, and predicted brain age difference (PBAD) descriptive statistics, as well as monozygotic (MZ) and dizygotic (DZ) twin pair polyserial correlations with associated 95% confidence intervals.

	Age (SD)	Total sample size	Complete twin pairs (MZ, DZ)	Singletons (MZ, DZ)	Mean	SD	$Corr_{MZ}$	$Corr_{DZ}$
Wave 1	56.2 (2.6)							
MD signature		365	90, 64	33, 24	−0.02	4.71	0.66 (0.52, 0.76)	0.21 (−0.04, 0.42)
Thickness/vol signature		499	126, 89	41, 28	0.01	3.47	0.68 (0.58, 0.76)	0.17 (−0.05, 0.37)
PBAD		508	128, 95	39, 23	−8.56	5.32	0.74 (0.65, 0.80)	0.37 (0.18, 0.53)
Wave 2	61.7 (2.6)							
MD signature		368	78, 52	58, 50	−0.09	4.28	0.73 (0.61, 0.80)	0.20 (−0.04, 0.42)
Thickness/vol signature		413	93, 67	53, 40	0.03	3.64	0.67 (0.53, 0.76)	0.42 (0.21, 0.59)
PBAD		421	96, 69	53, 38	−1.89	6.03	0.62 (0.50, 0.70)	0.22 (−0.003, 0.40)
Wave 3	67.6 (2.6)							
MD signature		316	52, 31	88, 62	0.01	4.45	0.63 (0.46, 0.75)	0.21 (−0.26, 0.55)
Thickness/vol signature		437	88, 54	87, 66	0.08	3.78	0.61 (0.46, 0.71)	0.47 (0.20, 0.66)
PBAD		513	122, 75	65, 54	1.59	5.47	0.66 (0.56, 0.74)	0.28 (0.04, 0.48)

Note: Of the 736 total participants included in the present analyses, 66, 87, and 81 participants met criteria for MCI at waves 1, 2, and 3, respectively. 4 participants at wave 3 were diagnosed with AD. The Jak-Bondi approach was used to diagnose mild cognitive impairment (MCI) in the sample (54, 55).

Biol Psychiatry Cogn Neurosci Neuroimaging. Author manuscript; available in PMC 2024 September 01.

Table 2.

Standardized variance components for best-fitting AE multivariate model.

	A	95% CI	E	95% CI
MD signature wave 1	0.56	(0.42, 0.68)	0.44	(0.24, 0.43)
MD signature wave 2	0.72	(0.61, 0.80)	0.28	(0.20, 0.39)
MD signature wave 3	0.62	(0.48, 0.72)	0.38	(0.28, 0.52)
Thickness/vol signature wave 1	0.66	(0.55, 0.74)	0.34	(0.25, 0.45)
Thickness/vol signature wave 2	0.69	(0.59, 0.76)	0.31	(0.24, 0.42)
Thickness/vol signature wave 3	0.64	(0.53, 0.72)	0.36	(0.28, 0.47)

Biol Psychiatry Cogn Neurosci Neuroimaging. Author manuscript; available in PMC 2024 September 01.

Table 3.

Correlations and 95% confidence intervals from best-fitting AE multivariate model.

Mean diffusivity (MD) and cortical thickness/volume signatures **additive genetic (below diagonal, bolded)** & *non-shared environmental (above diagonal, italicized)* correlations. Non-significant correlations are displayed in gray text.

	MD wave 1	MD wave 2	MD wave 3	Thickness/vol wave 1	Thickness/vol wave 2	Thickness/vol wave 3
MD wave 1	1	*0.34 (0.07, 0.55)*	*0.34 (−0.03, 0.63)*	*−0.14 (−0.32, 0.04)*	*−0.21 (−0.47, 0.08)*	*−0.25 (−0.51, 0.05)*
MD wave 2	**0.83 (0.69, 0.97)**	1	*0.26 (0.002, 0.51)*	*−0.11 (−0.34, 0.13)*	*−0.41 (−0.57, −0.23)*	*−0.32 (−0.51, −0.10)*
MD wave 3	**0.94 (0.76, 1.15)**	**0.98 (0.87, 1.10)**	1	*0.002 (−0.28, 0.27)*	*−0.27 (−0.46, −0.06)*	*−0.68 (−0.79, −0.52)*
Thickness/vol wave 1	**−0.37 (−0.53, −0.19)**	**−0.23 (−0.39, −0.06)**	**−0.20 (−0.40, −0.004)**	1	*0.39 (0.18, 0.56)*	*0.23 (−0.01, 0.45)*
Thickness/vol wave 2	**−0.69 (−0.85, −0.51)**	**−0.62 (−0.72, −0.49)**	**−0.56 (−0.71, −0.41)**	**0.78 (0.68, 0.87)**	1	*0.65 (0.51, 0.76)*
Thickness/vol wave 3	**−0.71 (−0.89, −0.53)**	**−0.58 (−0.72, −0.43)**	**−0.54 (−0.66, −0.39)**	**0.77 (0.63, 0.90)**	**0.85 (0.77, 0.93)**	1

Table 4.

Relationship between AD signatures and PBAD.

Phenotypic, genetic, and non-shared environmental correlations (and 95% confidence intervals) between measures from best-fitting AE trivariate model with the mean diffusivity (MD) signature, cortical thickness/volume signature, and predicted brain age difference (PBAD) scores.

		Phenotypic *r*	Genetic *r*	Non-shared environmental *r*
MD signature and PBAD	Wave 1	−0.49 (−0.56, −0.41)	−0.62 (−0.75, −0.48)	−0.27 (−0.44, −0.09)
	Wave 2	−0.55 (−0.62, −0.47)	−0.61 (−0.74, −0.46)	−0.44 (−0.60, −0.25)
	Wave 3	−0.54 (−0.61, −0.46)	−0.63 (−0.79, −0.47)	−0.42 (−0.59, −0.21)
Thickness/volume signature and PBAD	Wave 1	0.27 (0.18, 0.36)	0.35 (0.21, 0.49)	0.10 (−0.07, 0.26)
	Wave 2	0.51 (0.42, 0.58)	0.55 (0.40, 0.68)	0.42 (0.25, 0.57)
	Wave 3	0.51 (0.44, 0.58)	0.52 (0.38, 0.64)	0.50 (0.36, 0.63)

Table 5.

Pearson correlations (95% confidence intervals) between wave 1 individual regions in AD signatures with wave 3 cross-modality signatures. Results are presented for left and right hemisphere regions of interest (ROI).

Wave 1 mean diffusivity region of interest (ROI)	**Correlation with wave 3 cortical thickness/volume signature**	
	Left hemisphere ROI	***Right hemisphere ROI***
Entorhinal cortex	−0.17 (−0.31, −0.03)	−0.18 (−0.32, −0.05)
Middle temporal gyrus	−0.39 (−0.50, −0.26)	−0.38 (−0.50, −0.26)
Superior temporal gyrus	−0.39 (−0.50, −0.26)	−0.43 (−0.54, −0.30)
Bank of superior temporal sulcus	−0.37 (−0.49, −0.24)	−0.38 (−0.50, −0.26)
Isthmus cingulate	−0.22 (−0.35, −0.08)	−0.25 (−0.38, −0.12)
Lateral orbitofrontal cortex	−0.43 (−0.54, −0.31)	−0.32 (−0.44, −0.19)
Medial orbitofrontal cortex	−0.29 (−0.42, −0.16)	−0.24 (−0.37, −0.11)
Hippocampus	−0.16 (−0.29, −0.02)	−0.09 (−0.23, 0.05)
Wave 1 cortical thickness/volume region of interest (ROI)	**Correlation with wave 3 MD signature**	
	Left hemisphere ROI	***Right hemisphere ROI***
Entorhinal cortex	0.07 (−0.07, 0.21)	0.02 (−0.12, 0.16)
Middle temporal gyrus	−0.04 (−0.17, 0.11)	−0.08 (−0.22, 0.06)
Superior temporal gyrus	−0.20 (−0.33, −0.06)	−0.29 (−0.41, −0.16)
Bank of superior temporal sulcus	0.09 (−0.05, 0.23)	−0.01 (−0.15, 0.12)
Isthmus cingulate	−0.02 (−0.15, 0.12)	−0.08 (−0.21, 0.06)
Lateral orbitofrontal cortex	−0.10 (−0.23, 0.04)	−0.02 (−0.15, 0.12)
Medial orbitofrontal cortex	0.04 (−0.10, 0.18)	0.05 (−0.09, 0.19)
Hippocampus (volume)	−0.29 (−0.41, −0.16)	−0.26 (−0.38, −0.12)